

Ly α Driven Outflows Around Star Forming Galaxies

Mark Dijkstra^{*} & Abraham Loeb[†]

Harvard-Smithsonian Center for Astrophysics, 60 Garden Street, Cambridge, MA 02138, USA

11 March 2019

ABSTRACT

We present accurate Monte-Carlo calculations of Ly α radiation pressure in a range of models which represent galaxies during various epochs of our Universe. We show that the radiation force that Ly α photons exert on hydrogen gas in the neutral intergalactic medium (IGM), that surrounds minihalos that host the first stars, may exceed gravity by orders of magnitude and drive supersonic winds. Ly α radiation pressure may also dominate over gravity in the neutral IGM that surrounds the HII regions produced by the first galaxies. However, the radiation force is likely too weak to result in supersonic outflows in this case. Furthermore, we show that Ly α radiation pressure may drive outflows in the interstellar medium of star forming galaxies that reach hundreds of km s^{−1}. This mechanism could also operate at lower redshifts $z \lesssim 6$, and may have already been indirectly detected in the spectral line shape of observed Ly α emission lines.

Key words: cosmology: theory–galaxies: high redshift–radiation mechanisms: general–radiative transfer–ISM: bubbles

1 INTRODUCTION

HII regions around massive stars convert a significant fraction of the total bolometric luminosity of young galaxies into Ly α line emission (Partridge & Peebles 1967; Schaerer 2003). This Ly α radiation can exert a large force on surrounding neutral gas, as the Ly α transition has a cross-section that is ~ 7 orders of magnitude larger than the Thomson cross-section, when averaged over a frequency band as wide as the resonance frequency itself (e.g. Loeb 2001). Not surprisingly, the impact of Ly α radiation pressure on the formation of galaxies has been discussed extensively (e.g. Cox 1985; Elitzur & Ferland 1986; Bithell 1990; Haehnelt 1995; Oh & Haiman 2002; McKee & Tan 2007), but the intricacies of Ly α radiative transfer in 3D complicated an accurate numerical treatment of its dynamical effect on the gas. Nevertheless, an approximate estimate can be obtained from simple energy considerations as shown below.

Consider a self-gravitating gas cloud of total (baryons + dark matter) mass M and radius R that contains a central Ly α source. The gravitational binding energy of the baryons inside the cloud, $E_B \sim \Omega_b GM^2/(\Omega_m R)$, can be compared to the total energy in the Ly α radiation field inside the cloud, $E_\alpha = L_\alpha \times t_{\text{trap}}$. Here, L_α is the Ly α luminosity of the central source (in erg s^{−1}), and t_{trap} is the typical trapping time of Ly α photons in the cloud owing to

scattering on hydrogen atoms. The Ly α radiation pressure would unbind the baryonic gas from the cloud if $E_\alpha > E_B$, i.e. $L_\alpha > \Omega_b GM^2/(\Omega_m R t_{\text{trap}})$ (e.g. Cox 1985; Bithell 1990; Oh & Haiman 2002). In this approach, t_{trap} is one of the key parameters in setting the Ly α radiation pressure. Calculations by Adams (1975) imply that $t_{\text{trap}} \sim 15 t_{\text{light}}$ for $3 \lesssim \log \tau_0 \lesssim 5.5$, and $t_{\text{trap}} \sim 15(\tau_0/10^{5.5})^{1/3} t_{\text{light}}$ otherwise, for a static, uniform, infinite slab of material (also see Fig 1 of Bonilha et al. 1979). Here τ_0 is the line center optical depth from the center to the edge of the slab, and t_{light} is the light crossing time if the medium were transparent (i.e. $t_{\text{light}} = R/c$ in the case of the cloud described above). Note however, that the precise value of t_{trap} depends on other factors including for example, the gas distribution (clumpiness and geometry), the velocity distribution of the gas, and the dust content of the cloud (Bonilha et al. 1979). The Ly α radiation pressure becomes comparable to gravity when

$$L_{\alpha,41} = 1.0 \left(\frac{M}{10^8 M_\odot} \right)^{4/3} \left(\frac{16}{1+z} \right)^2 \left(\frac{15 t_{\text{light}}}{t_{\text{trap}}} \right), \quad (1)$$

where $L_\alpha = L_{\alpha,41} \times 10^{41}$ erg s^{−1}, and where we have substituted the virial radius of a galaxy mass M , $R_{\text{vir}} = 0.97 \text{ kpc} \times (M/10^8 M_\odot)^{1/3} (1+z/16)^{-1}$, for R (Eq. 24 of Barkana & Loeb 2001). For comparison, a star forming galaxy can generate a Ly α luminosity of $L_\alpha = (10^{42} - 10^{43}) \times (\text{SFR}/M_\odot \text{ yr}^{-1}) \text{ erg s}^{-1}$, where the precise conversion factor depends on the gas metallicity and the stellar initial mass function (e.g. Schaerer 2003). Therefore, a star formation rate of merely $\text{SFR} \gtrsim 0.01 - 0.1 M_\odot \text{ yr}^{-1}$ is needed to gener-

^{*} E-mail: mdijkstr@cfa.harvard.edu

[†] E-mail: aloeb@cfa.harvard.edu

ate a Ly α luminosity that is capable of unbinding gas from a halo of mass $10^8 - 10^9 M_\odot$.

Halos of $\lesssim 10^9 M_\odot$ are very common at $z \gtrsim 6$, and have a sufficiently large reservoir of baryons to sustain the above-mentioned star formation rates for a prolonged time. In this paper we provide a more detailed investigation of the magnitude of Ly α radiation pressure in the environment of high-redshift star forming galaxies. In particular, we use a Ly α Monte-Carlo radiative transfer code (Dijkstra et al. 2006) to compute Ly α radiation pressure in a wider range of models. Our treatment of radiative transfer and our focus on the environment of high-redshift star forming galaxies, distinguish this paper from previous work. We will show that the radiation force exerted by Ly α photons on neutral hydrogen gas can exceed the gravitational force that binds the gas to its host galaxy by orders of magnitude, and may drive supersonic outflows of neutral gas both in the intergalactic and the interstellar medium.

The outline of this paper is as follows. In § 2 we describe how Ly α radiation pressure is computed in the Monte-Carlo radiative transfer code, and show the tests that are performed to test the accuracy of the code. In § 3, we present our numerical results. Finally, § 4 summarizes the implications of our work and our main conclusions. The cosmological parameter values used throughout our discussion are $(\Omega_m, \Omega_\Lambda, \Omega_b, h) = (0.27, 0.73, 0.042, 0.70)$ (Komatsu et al. 2008).

2 LY α RADIATION PRESSURE

The force F_{rad} experienced by an atom in a direction \mathbf{n} is related to the flux through a plane normal to \mathbf{n} ,

$$F_{\text{rad}} = \frac{4\pi}{c} \int d\nu \sigma(\nu) H(\nu), \quad (2)$$

where $\sigma(\nu)$ is the Ly α absorption cross-section at frequency ν . The specific flux is given by $H(\nu) = \frac{1}{2} \int d\mu \mu I(\mu, \nu)$, where $I(\nu, \mu)$ is the specific intensity of the radiation field (see, e.g. Eq. 1.113 in Rybicki & Lightman 1979), and $\mu = \mathbf{n} \cdot \mathbf{k}$ in which \mathbf{k} denotes the propagation direction of the radiation (i.e. $\mu = 1$ for radiation propagating perpendicular to the plane).

The specific intensity obeys the radiative transfer equation, which reads (in spherical coordinates)

$$\mu \frac{\partial I}{\partial r} + \frac{(1 - \mu^2)}{r} \frac{\partial I}{\partial \mu} = \chi_\nu (J - I) + S_\nu(r), \quad (3)$$

where in this equation $\mu \equiv \mathbf{r} \cdot \mathbf{k}/|\mathbf{r}|$, $J(\nu) = \int d\mu I(\mu, \nu)$ denotes the mean intensity, χ_ν denotes the opacity at frequency ν , and $S_\nu(r)$ the emission function for newly created photons at frequency ν and radius r (in photons $\text{cm}^{-3} \text{s}^{-1} \text{sr}^{-1} \text{Hz}^{-1}$; see e.g. Loeb & Rybicki 1999). Under the assumption that $I(\nu, \mu)$ has only a weak dependence on direction (which is reasonable given that Ly α radiation scatters very frequently), $I(\nu, \mu)$ can be expressed as a first-order Taylor expansion in μ , i.e. $I(\nu, \mu) = a(\nu) + b(\nu)\mu$. In this so-called ‘‘Eddington approximation’’, the expression for flux simplifies to (e.g. Rybicki & Lightman 1979, their Eq. 1.118)

$$H(\nu) = \frac{1}{3} \frac{dJ(\nu)}{d\tau} = \frac{c}{12\pi} \frac{du(\nu)}{d\tau}, \quad (4)$$

where $d\tau = \chi_\nu dr = n_H \sigma(\nu) dr$ with n_H being the number density of neutral hydrogen atoms, and $u(\nu)$ is the specific energy density in the radiation field at a frequency ν . Here we have used the relation, $u = 4\pi J/c$. Substituting this expression back into Eq. (2) yields

$$F_{\text{rad}} = \frac{1}{3n_H} \frac{d}{dr} \int d\nu u(\nu) = \frac{1}{3n_H} \frac{dU}{dr}, \quad (5)$$

where we defined $U \equiv \int d\nu u(\nu)$. Note that the cross-section does not appear in the final expression for the radiation force¹.

2.1 Implementation in Monte-Carlo Technique

In our Monte-Carlo simulation we sample the gas density and velocity fields with $N_s = 5000$ concentric spherical shells. The radius, thickness, and volume of shell j are denoted by r_j , dr_j , and V_j , respectively. We compute the radiation force using two approaches:

- In the first approach, we calculate the energy density (U in Eq. 5) in the Ly α radiation field as a function of radius: Using the Monte-Carlo simulation we compute the average time that photons spend in shell j , which we denote by $\langle t \rangle_j$. The total number of photons that is present in shell j at any given time is then given by $N_{\alpha,j} = \dot{N}_\alpha \times \langle t \rangle_j$, where \dot{N}_α is the rate at which photons are emitted. This yields the energy density, $U_j = N_{\alpha,j} h\nu_\alpha / V_j$. Finally, Eq. (5) is used to compute the radiation force on atoms in shell j .

- In the second approach, we calculate the momentum transfer from a Ly α photon to an atom in each scattering event, $\Delta p = h_p(\mathbf{k}_{\text{in}} - \mathbf{k}_{\text{out}})/2\pi$, where h_p is Planck’s constant. Here, \mathbf{k}_{in} and \mathbf{k}_{out} are the photons wavevectors before and after scattering. We compute the average *total momentum transfer* (i.e. summed over all scattering events) per photon in shell j , $\langle \Delta \mathcal{P} \rangle_j$, and obtain the total momentum transfer from $\dot{P}_{\alpha,j} = \dot{N}_\alpha \times \langle \Delta \mathcal{P} \rangle_j$. The force on an individual atom is obtained by dividing by the total number of hydrogen atoms in shell j , i.e. $F_j = \dot{P}_{\alpha,j} / (V_j \times n_{H,j})$.

Both methods should give identical results, provided that the Eddington approximation holds.

2.2 Test Case: Sources in a Neutral Comoving IGM

We begin by considering a Ly α point source at a redshift $z = 10$ embedded in a neutral intergalactic medium (IGM) that is expanding with the Hubble flow. The photons scatter and diffuse away from the source while Hubble expansion redshifts the photons away from resonance. In this case, the angle-averaged intensity $J(\nu)$ and its radial dependence can be calculated analytically (Loeb & Rybicki 1999). The availability of analytic expressions for $J(\nu, r)$, and therefore the radiation force F_{rad} (through Eq. 5), makes this a good test case for our code.

In Figure 1 we plot the radial dependence of the energy density (in erg cm^{-3}) in the Ly α radiation field for a

¹ The right-hand-side of Eq. (5) is analogous to the usual pressure gradient force in fluid-dynamics which is not dependent on the scattering cross-section of the fluid particles.

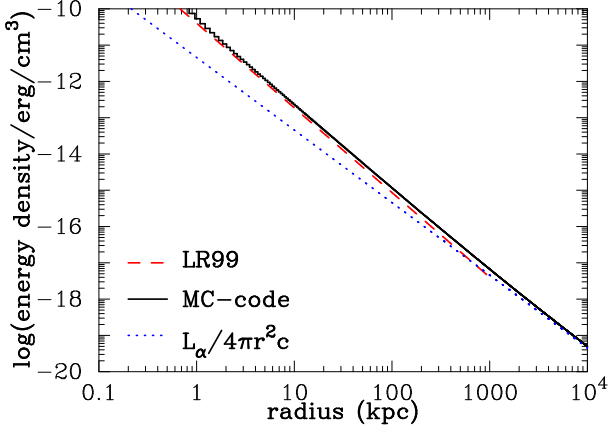


Figure 1. Radial profile of the energy density $U(r)$ (erg cm^{-3}) in the Ly α radiation field surrounding a central source that is emitting 10^{54} photons s^{-1} into an expanding neutral IGM. The blue dotted line shows $U(r)$ if the IGM were fully transparent. The black solid (red dashed) line shows $U(r)$ when radiative transfer is included using an analytic (Monte-Carlo) approach (see text). Scattering reduces the speed at which Ly α photons are propagating radially outward, increasing $U(r)$ relative to the transparent case.

model in which the central source is emitting 10^{54} photons s^{-1} . This corresponds to a luminosity of $L_\alpha = 1.6 \times 10^{43}$ erg s^{-1} , which represents a bright Ly α emitting galaxy (e.g. Ouchi et al. 2008). The blue dotted line shows the energy density if the IGM were fully transparent to Ly α radiation. In this hypothetical case all photons stream radially outward, and the energy density is given by $L_\alpha / (4\pi r^2 c)$. The red dashed line shows the energy density, $U(r) = \frac{4\pi}{c} \int d\nu J(\nu, r)$, derived from the analytic expression for $J(r, \nu)$ given in Loeb & Rybicki (1999, their Eq. 21), while the black histogram shows the energy density extracted from the simulation (§ 2.1). Clearly, the analytic and Monte-Carlo calculations yield consistent results. Scattering reduces the effective speed at which photons propagate radially outward, which enhances their energy density (especially at small radii) relative to the transparent case. At sufficiently large distances however, the photons have redshifted far enough from resonance that they are propagating almost freely to the observer, and the energy density approaches $L_\alpha / 4\pi r^2 c$.

In Figure 2 we compare the radiation force to the gravitational force on a single hydrogen atom, $F_{\text{grav}} = GM(<r)m_p/r^2$, where $M(<r)$ is the total mass enclosed within a radius r . We plot the ratio $F_{\text{rad}}/F_{\text{grav}}$ scaled by $M = 10^{11} M_\odot$ ². The black dotted line (grey solid histogram) was calculated by applying Eq. (5) to the energy density $U(r)$ that was obtained by using the analytic (Monte-Carlo) approach (also see Fig 1). For comparison, the black solid histogram was obtained by directly computing the momentum transfer rate from photons to atoms as outlined in § 2.1. Figure 2 shows that the radiation force overwhelms gravity at small radii. The energy density scales approximately as

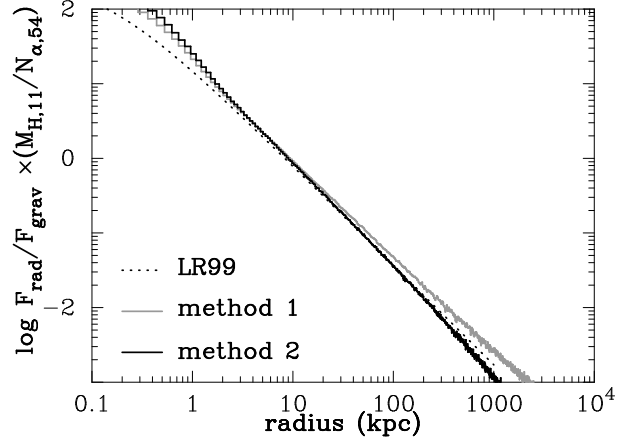


Figure 2. The ratio of radiation to gravitational force on a hydrogen atom as a function of physical radius in kpc. To scale out the dependence of this ratio on halo mass, M_h , and production rate of Ly α photons by the central source, \dot{N}_α , the vertical axis is normalized by $M_{h,11}/\dot{N}_{\alpha,54}$ (see text). The black dotted (grey solid) line was obtained by applying Eq. (5) to the energy density $U(r)$ that was obtained by using the analytic (Monte-Carlo) approach (see Fig 1). The black solid line was obtained by directly computing the momentum transfer rate from photons to atoms in the Monte-Carlo code as outlined in § 2.1. The results demonstrate that (i) the radiation force exceeds gravity at $r < 10(\dot{N}_{\alpha,54}/M_{h,11})$ kpc, and (ii) both methods yield consistent results.

$\partial \log U / \partial \log r \sim -2.3$ (Fig 1). Therefore, $F_{\text{rad}}/F_{\text{grav}} \propto r^{-1.3}$ and reaches unity at $r \sim 10$ physical kpc.

The radiation force increases linearly with \dot{N}_α while the gravitational force scales as M . Thus, $F_{\text{rad}}/F_{\text{grav}}$ scales linearly with the ratio $\mathcal{R} \equiv \dot{N}_\alpha/M$. To scale out the dependence on \mathcal{R} , the vertical axis shows the quantity $(F_{\text{rad}}/F_{\text{grav}}) \times (M_{11}/\dot{N}_{\alpha,54})$, where $\dot{N}_{\alpha,54} \equiv (\dot{N}_\alpha/10^{54} \text{ photons s}^{-1})$ and $M_{11} = (M/10^{11} M_\odot)$. For example, if $M_{11} = 0.1$ then Figure 2 shows that radiation pressure exceeds gravity out to $r = 100$ kpc, well beyond the virial radius of a halo of this mass at $r_{\text{vir}} \sim 6.6$ kpc.

Most importantly, Figure 2 shows that the two approaches used to compute the radiation force in the simulation yield consistent results, with a noticeable deviation only at the largest radii ($r \sim 1$ Mpc). At large radii most photons stream outwards radially and the Eddington approximation that was used to derive Eq. (4) becomes increasingly unreliable.

Next, we use the radiative transfer code to explore the magnitude of the Ly α radiation pressure for a range of models which represent an evolutionary sequence of structure formation in the Universe. We focus on the Ly α radiation pressure on gas surrounding (i) the first stars (§ 3.1); (ii) the first galaxies (§ 3.2); and (iii) the interstellar medium of galaxies (§ 3.3).

3 RESULTS

3.1 Case I: A Single Massive Star in a Minihalo

Numerical simulations of structure formation suggest the first stars that formed in our Universe were massive ($M_\star \sim 100 M_\odot$), and formed as single objects in dark matter halos

² The number density of halos more massive than $10^{11} M_\odot$ at $z = 10$ is $\sim 10^{-7}$ comoving Mpc^{-3} , implying that these rare halos are among the most massive ones in existence at that early cosmic time.

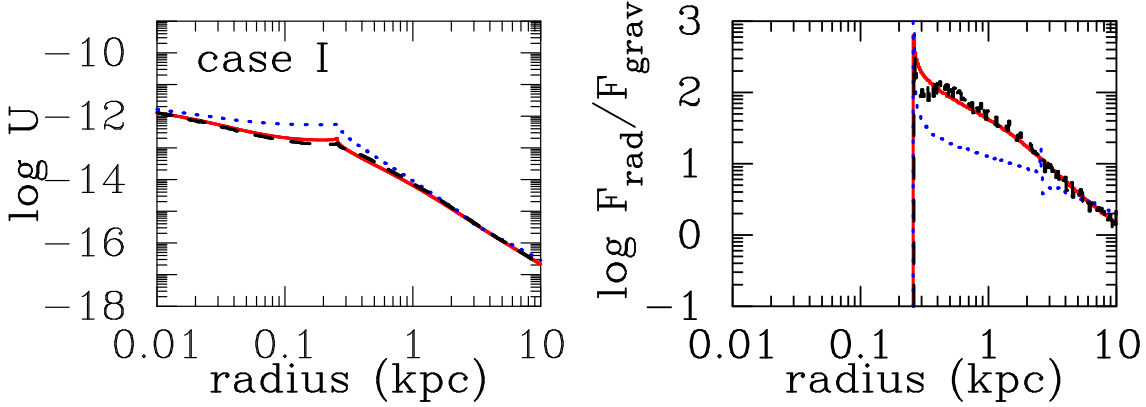


Figure 3. The energy density in the Ly α radiation field (*left panel*), and the ratio between the radiation and the gravitational forces (*right panel*) for a single very massive star ($M_* = 100M_\odot$) in a minihalo $M_h = 2 \times 10^6 M_\odot$. The star ionizes all the gas out to the virial radius at $r = 0.26$ kpc. Ly α photons freely propagate until they reach the edge of the HII region, where they are likely to be scattered back into the ionized minihalo. This yields an almost constant radiation energy density. Once outside the HII region, the radiation force dominates over gravity out to $r = 10$ kpc and may accelerate neutral gas outside the HII region to velocities of order ~ 10 km s $^{-1}$.

with masses of $M \sim 10^6 M_\odot$ that collapsed at $z > 10$ (e.g. Haiman et al. 1996; Abel et al. 2002; Yoshida et al. 2006). Here, we focus our attention on a star with a mass $M_* = 100M_\odot$ that formed at $z = 15$ in a dark matter mini-halo of mass $M = 2 \times 10^6 M_\odot$. The star emits 10^{50} ionizing photons per second (Schaerer 2002; Abel et al. 2007). We assume that the ionizing flux ionizes all the gas out to the virial radius of the dark matter halo ($r_{\text{vir}} = 0.26$ kpc) but not beyond that radius (Kitayama et al. 2004). Hence, the IGM gas surrounding this central source is assumed to be neutral ($x_{\text{HI}} = 1.0$) and cold ($T_{\text{gas}} = 300\text{K}$, which corresponds to the temperature of the neutral IGM at $z = 15$ due to X-Ray heating, see e.g. Fig 1 of Pritchard & Loeb 2008).

Recombination following photoionization converts $\sim 68\%$ of all ionizing photons into Ly α photons (Osterbrock 1989, p 387). Hence, the entire halo is a Ly α source that is surrounded by neutral intergalactic gas. To determine the radial dependence of the Ly α production rate (S_ν in Eq. 3), we need to specify the gas density profile. We assume that the gas distribution inside the dark matter halo is described by an NFW-profile with a concentration parameter $C = 5$ and a thermal core³ at $r < 3r_{\text{vir}}/4C$ (see Maller & Bullock 2004). We point out however, that our final results are not sensitive to our choice of $S_\nu(r)$.

Once $S_\nu(r)$ has been determined, we find the radius, r , at which a Ly α photon is generated in the Monte-Carlo simulation from the relation

$$R = \frac{1}{N} \int_0^r dr 4\pi r^2 n_{\text{H}}^2 \alpha_{\text{rec}}, \quad (6)$$

where R is a random number between 0 and 1, $N = \int_0^{r_{\text{vir}}} dr 4\pi r^2 n_{\text{H}}^2 \alpha_{\text{rec}}$ is the total recombination rate inside the dark matter halo, and $\alpha_{\text{rec}} = 2.6 \times 10^{-13} \text{ cm}^3 \text{ s}^{-1}$ is the case-B recombination coefficient at a temperature $T = 10^4$ K (e.g. Hui & Gnedin 1997). Once the photon is generated,

it scatters through the neutral IGM until it has redshifted far enough from resonance that it can escape to the observer.

In the *left panel* of Figure 3 we show the energy density (in erg cm^{-3}) of the Ly α radiation field as a function of radius. The *red solid line* represents a model in which we assumed the IGM to follow the mean density and Hubble expansion right outside the virial radius. The *blue dotted line* shows a more realistic model in which the IGM is still over-dense near the virial radius, and in which the intergalactic gas is gravitationally pulled towards the minihalo (see Dijkstra et al 2007 for a quantitative description of the density and velocity profiles based on the model of Barkana 2004). The *black dashed line* shows the same model as the *red solid line* but with the neutral fraction increasing linearly between r_{vir} and $2r_{\text{vir}}$. This provides a better representation of the fact that the central population III star emits ionizing photons with energies $\gtrsim 54$ eV, which can photoionize hydrogen (and helium) atoms that lie deeper in the IGM. The goal of this model is to investigate whether our results depend sensitively on the presence of a sharp boundary between HI and HII.

All models show that the radiation energy density within the fully ionized minihalo ($r \lesssim r_{\text{vir}} = 0.26$ kpc) has only a weak dependence on radius, i.e. $d \log U / d \log r \gtrsim -1$. Naively, this may appear surprising given the fact that within the model, no scattering occurs within the virial radius and one may expect the energy density in the Ly α radiation field to scale as $U \propto r^{-2}$. However, in reality U obtains only a weak radial dependence because the radiation can be scattered back into the ionized minihalo as soon as it ‘hits’ the wall of neutral IGM gas. Ly α photons are therefore trapped inside the ionized minihalo and their energy density is boosted to a value that is only weakly dependent on radius. On the other hand, for $r \gtrsim r_{\text{vir}}$ we find that $d \log U / d \log r \lesssim -2$, which is because Ly α photons are trapped more efficiently near the edge of the HII region, while they stream freely outwards at larger radii (as in § 2.2 and Fig 1). Figure 3 shows clearly that the radial dependence of the Ly α energy density is not sensitive to the detailed model assumptions about the gas in the IGM.

In the *right panel* of Figure 3 we show the ratio be-

³ With this gas density profile, the total recombination rate inside the dark matter halo is $\int_0^{r_{\text{vir}}} dr 4\pi r^2 n_{\text{H}}^2 \alpha_{\text{rec}} \sim 4.5 \times 10^{49} \text{ s}^{-1}$. The total recombination rate can be increased to balance the photoionization rate by introducing a clumping factor $K \equiv \langle n_{\text{H}}^2 \rangle / \langle n_{\text{H}} \rangle^2 \sim 2$.

tween the radiation force (Eq. 5) and the gravitational force on a single hydrogen atom), $F_{\text{grav}} = GM(< r)m_p/r^2$, where $M(< r)$ is the total (baryons + dark matter) mass enclosed within a radius r . In all models, radiation pressure dominates over gravity by as much as $\gtrsim 2$ orders of magnitude. The radiation force is largest for the models in which the IGM is assumed to be at mean density, because of the n_{H}^{-1} factor in the equation for the radiation force (Eq. 5). Note that the spike near $r \sim 2.6$ kpc for the other two models is due to an artificial discontinuity in the IGM velocity field that exists in this model.

Ly α radiation pressure may operate throughout the lifetime of the central star. Over a lifetime of ~ 2.5 Myr (see Table 4 of Schaerer 2002), this mechanism is capable of accelerating the gas to velocities of 10 (50) km s $^{-1}$ at $r = 0.3$ kpc in the model represented by the *blue dotted (red solid) line*, and to 4 (16) km s $^{-1}$ at $r = 0.4$ kpc (the reason for this large difference is that the edge of the HII region lies at $r = 0.26$ kpc. Hence, gas at $r = 0.3$ kpc is separated by 0.04 kpc from this edge, while gas at $r = 0.4$ kpc is separated by a distance that is 3.5 times larger).

Thus, Ly α radiation pressure can accelerate the gas to velocities that exceed the escape velocity from the dark matter halo ($v_{\text{esc}} \sim \sqrt{2}v_{\text{circ}} \sim 8$ km s $^{-1}$) as well as the sound speed of the intergalactic medium ($c_s = 2.2(T_{\text{gas}}/300 \text{ K})^{1/2}$ km s $^{-1}$).

Note that as the gas is pushed out and its velocity profile changes, the subsequent radiative transfer is altered. For example, we repeated the radiative transfer calculation for models in which gas at $r_{\text{vir}} < r \lesssim 2r_{\text{vir}}$ was accelerated to velocities in the range 10 – 20 km s $^{-1}$ (outward) and found a slightly shallower profile for $U(r)$ which lowered the radiation force by a factor of ~ 3 . Consequently, the acceleration of the gas decreases with time and the actual velocities reached by the gas are lower than the estimates given above by a factor of a few. Nevertheless, the resulting velocities are still substantial.

Our calculations imply that Ly α radiation pressure can affect the gas dynamics in the IGM surrounding minihalos that contain the first stars. The impact of Ly α radiation pressure increases with decreasing density of the surrounding gas in the IGM. In practice, the distribution of the IGM is not spherically symmetric. Instead, the density is expected to vary from sightline to sightline (being large along filaments and small along voids). Our results imply that Ly α radiation pressure will be most efficient in ‘blowing out’ the lower density gas. This conjecture is supported by the tendency of Ly α photons to preferentially scatter through the low-density gas; their propagation along the path of least resistance would naturally boost up the Ly α flux there. This effect will be moderated by the tendency of the HII region around the first stars to extend further into the low density gas (in ‘butterfly’-like patterns, e.g. Abel et al, 1999).

If the central star dies in a supernova explosion, then the resulting violent outflow could blow most of the baryons out from the minihalo. However, stars with masses in the range $30M_{\odot} \lesssim M_{\star} \lesssim 140M_{\odot}$ and $M_{\star} \gtrsim 260M_{\odot}$, are not expected to end their lives in a supernova. Instead, these stars collapse directly to a black hole (Heger & Woosley 2002) and have weak winds (because of the lack of heavy elements in their atmosphere), so that radiation pressure may be the dominant process that affects their surrounding IGM.

In summary, Ly α radiation pressure on the neutral IGM around minihalos in which the first stars form, can exceed gravity by orders of magnitude and launch supersonic winds. Our limited analysis does not allow a detailed discussion on the consequences of these winds. This requires 3D simulations with cosmological initial conditions that capture the full IGM density field around the minihalo and that track the evolution of the shocks that may form in the IGM. Such simulation are numerically challenging as they require self-consistent treatment of gas dynamics and Ly α radiative transfer in a moving inhomogeneous medium.

3.2 Case II: A Young Star Forming Galaxy

Our second case concerns a young galaxy that is forming multiple stars in a dark matter halo of mass $M = 10^9 M_{\odot}$ at $z = 10$. We assume that the galaxy is converting a fraction $f_{\star} = 10\%$ of its baryons into stars over $\sim 0.1t_{\text{H}}$ (Wyithe & Loeb 2006), where $t_{\text{H}} = [2/3H(z)] \sim 0.49$ Gyr, is the age of the Universe at $z = 10$. This translates to a star formation rate of $\dot{M}_{\star} = 0.34M_{\odot} \text{ yr}^{-1}$. For population III stars forming out of pristine gas, the total emission rate of ionizing photons is $\dot{N}_{\text{ion}} \sim 3 \times 10^{53} \text{ s}^{-1}$ (Schaerer 2002)⁴. If $\sim 1\%$ of the ionizing photons escape from the galaxy (Chen et al. 2007; Gnedin et al. 2008), then this translates to a Ly α luminosity of $L_{\alpha} = 3 \times 10^{42} \text{ erg s}^{-1}$. Furthermore, this galaxy can photoionize a spherical HII region of a radius $R_{\text{HII}} \sim 50$ physical kpc. Note however, that other ionizing sources would likely exist within this HII region. Indeed, clusters of sources are thought to determine the growth of ionized bubbles during reionization. This results in a characteristic HII region size that is significantly larger than that produced by single source, especially during the later stages of reionization (e.g. Furlanetto et al. 2004; McQuinn et al. 2007). In this framework, our model represents a star forming galaxy during the early stages of reionization or alternatively a galaxy that lies 50 kpc away from the edge of a larger ionized bubble.

In this particular case, the majority of all recombination events occur in the central galaxy. Thus, we initiate all Ly α photons at $r = 0$ in the Monte-Carlo simulation. We assume that the gas is completely ionized out to $R_{\text{HII}} = 50$ kpc, beyond which it is neutral. As shown in § 3.1, this abrupt transition in the ionized fraction of H in the gas does not affect our results.

The *left panel* of Figure 4 shows the energy density (in erg cm $^{-3}$) of the Ly α radiation field as a function of radius. The *solid line* represents the model discussed above. A kink in the energy density is seen at the edge of the HII region (see § 3.1 for a more detailed discussion of the profile). The *dotted line* represents a variant of the model in which we have reduced the size of the HII region to $R_{\text{HII}} = 20$ kpc.

The *right panel* of Figure 4 shows the ratio between the radiation and the gravitational forces on a single hydrogen atom. In our fiducial model, the radiation force does not exceed gravity; rather, at the edge of the HII region, gravity

⁴ More precisely, the ionizing photon production rate is $\sim 10^{54} \text{ s}^{-1} \times (\text{SFR}/M_{\odot} \text{ yr}^{-1})$ in the no-mass-loss model of Schaerer (2002) in which metal-free stars form according to a Salpeter IMF with $M_{\text{low}} = 1M_{\odot}$ and $M_{\text{high}} = 500M_{\odot}$ (his model ‘B’).

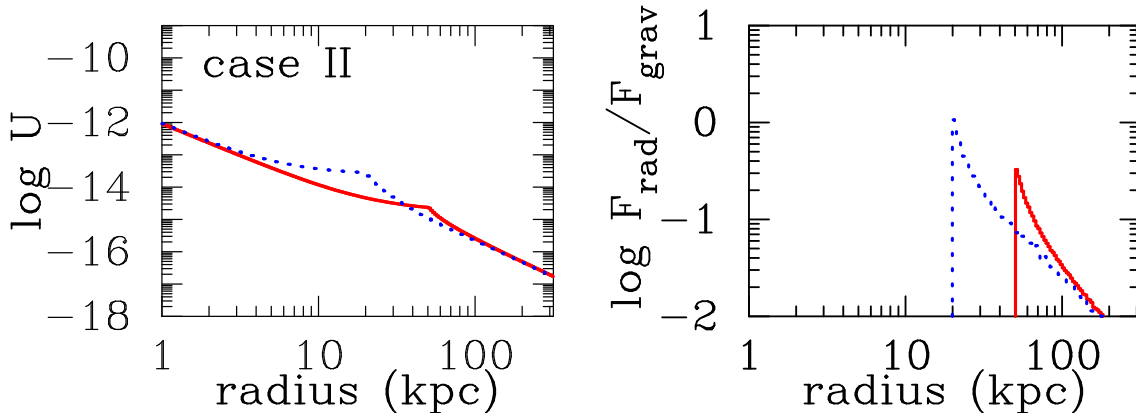


Figure 4. Same as Figure 3, but for the case of a star forming galaxy ($\dot{M}_* = 0.34 M_\odot \text{ yr}^{-1}$, see text), surrounded by an HII region with a radius $R_{\text{HII}} = 50$ kpc ($R_{\text{HII}} = 20$ kpc) for the *solid line* (*dotted line*), which is in turn surrounded by a fully neutral intergalactic medium (IGM). For the assumed total halo mass of $M_{\text{tot}} = 10^9 M_\odot$, the pressure exerted by the Ly α photons is not large enough to exceed gravity. However, radiation pressure wins for $M_{\text{tot}} = 10^8 M_\odot$, but even in this case the radiation force is not large enough to produce a significant wind speed in the IGM (see text).

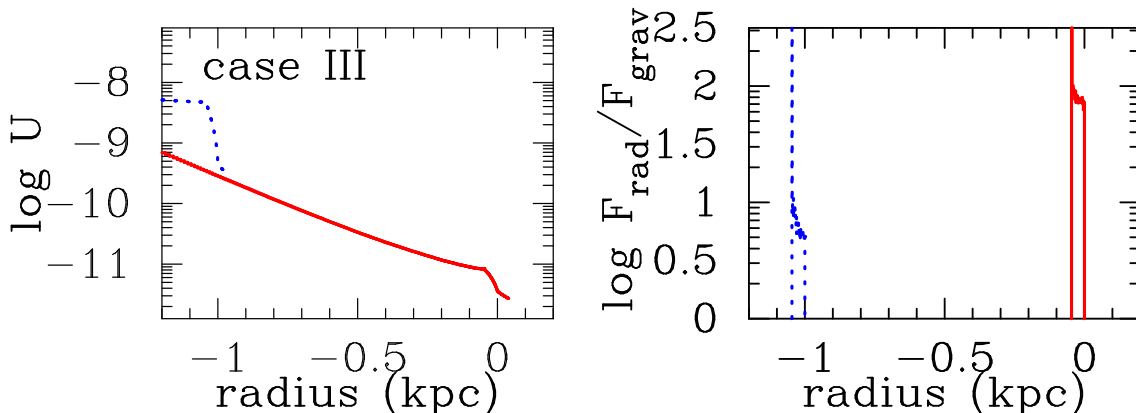


Figure 5. Same as in Figure 3 and Figure 4, but for models in which a central Ly α source of luminosity L_α is surrounded by a thin ($r_{\text{sh,min}} = 0.9 r_{\text{sh,max}}$) spherical shell of HI that is expanding at $v_{\text{sh}} = 200 \text{ km s}^{-1}$. The *blue dotted lines* (*red solid lines*) represent a model in which $N_{\text{HI}} = 10^{21} \text{ cm}^{-2}$ and $r_{\text{sh,max}} = 0.1$ kpc ($N_{\text{HI}} = 10^{19} \text{ cm}^{-2}$ and $r_{\text{sh,max}} = 1.0$ kpc). When calculating F_{grav} , we assumed the total mass enclosed by the supershell to be $10^8 M_\odot$ (see text). The results strongly suggest that Ly α radiation pressure may be dynamically important in the interstellar medium of galaxies. The *total* radiation force on the shell (obtained as a sum over all atoms) may be computed via $F_{\text{tot}} = M_F L_\alpha / c$, where M_F may be thought of as a force multiplication factor that depends both on the shell's outflow speed, v_{exp} , and its HI column density, N_{HI} . The dependence of M_F on these parameters is shown in Fig 6.

is ~ 3 times stronger. The radiation force becomes equal to the gravitational force if $R_{\text{HII}} = 20$ kpc. This requires an extremely low [by a factor $\sim (50/20)^3$] escape fraction of ionizing photons, $f_{\text{esc}} \sim 6 \times 10^{-4}$.

Alternatively, radiation pressure *is* important when the halo mass of the star forming region is reduced to $10^8 M_\odot$. Halos of this mass are the the most abundant halos at $z \sim 10$ that are capable of cooling via excitation of atomic hydrogen (i.e. their virial temperature just exceeds $T_{\text{vir}} \sim 10^4$ K, e.g. Barkana & Loeb 2001). The total gas reservoir inside these halos is $M_b = \frac{\Omega_b}{\Omega_m} M_{\text{tot}} \sim 1.5 \times 10^7 M_\odot$, and so these halos can sustain a star formation rate of $\dot{M}_* = 0.3 M_\odot \text{ yr}^{-1}$ for up to ~ 50 Myr. However, even if the radiation force is allowed to operate for ~ 50 Myr, we find that radiation pressure cannot accelerate the gas in the IGM to velocities that exceed $\sim 1 \text{ km s}^{-1}$. We therefore conclude that although Ly α pressure may exceed gravity in the neutral IGM that surrounds HII regions around $M_{\text{tot}} = 10^8 M_\odot$ halos, the ab-

solute magnitude of the radiation force is too weak to drive the IGM to supersonic velocities.

3.3 Case III: Ly α Driven Galactic Supershells

In principle, Ly α radiation pressure can be important when neutral gas exists in close proximity to a luminous Ly α source. So far, we focused our attention on HI gas in the IGM. However, neutral gas in the interstellar medium (ISM) of the host galaxy is located closer to the Ly α sources and should be exposed to an even stronger Ly α radiation pressure. Indeed, it has been demonstrated (e.g. Ahn & Lee 2002; Verhamme et al. 2008) that scattering of Ly α photons by neutral hydrogen atoms in a thin (with a thickness much smaller than its radius), outflowing 'supershell' of HI gas surrounding the star forming regions can naturally explain two observed phenomena: (i) the common shift of the Ly α emission line towards the red relative to other nebular

recombination and metal absorption lines (e.g. Pettini et al. 2001; Shapley et al. 2003); and (ii) the asymmetry of the Ly α line with emission extending well into its red wing (e.g. Lequeux et al. 1995).

The existence of thin, outflowing shells of neutral atomic hydrogen around HII regions is confirmed by HI-observations of our own Milky-Way (Heiles 1984) and other nearby galaxies (e.g. Ryder et al. 1995). The largest of these shells, so-called ‘supershells’, have radii of $r_{\text{max}} \sim 1$ kpc (e.g. Ryder et al. 1995; McClure-Griffiths et al. 2002) and HI column densities in the range $N_{\text{HI}} \sim 10^{19} - 10^{21} \text{ cm}^{-2}$ (e.g. Lequeux et al. 1995; Kunth et al. 1998; Verhamme et al. 2008). Supershells are thought to be generated by stellar winds or supernovae explosions which sweep-up gas into a thin expanding neutral shell (see e.g. Tenorio-Tagle & Bodenheimer 1988, for a review). The back-scattering mechanism attributes both the redshift and asymmetry of the Ly α line to the Doppler boost that Ly α photons undergo as they scatter off the outflow on the far side of the galaxy back towards the observer (e.g. Lee & Ahn 1998; Ahn & Lee 2002; Ahn et al. 2003; Ahn 2004; Verhamme et al. 2006, 2008). It is interesting to investigate whether Ly α radiation pressure may provide an alternative mechanism that determines the supershell kinematics.

In Figure 5 we show the energy density (*left panel*) and the Ly α radiation force (*right panel*) for two models. Both models assume that: (i) there is a Ly α source at $r = 0$ with a luminosity of $L_{\alpha} = 10^{43} \text{ erg s}^{-1}$; (ii) the emitted Ly α spectrum prior to scattering has a Gaussian shape as a function of photon frequency with a Doppler velocity width of $\sigma = 50 \text{ km s}^{-1}$; (iii) the spatial width of the supershell is 10% of its radius; and (iv) the shell has an outflow velocity of $v = 200 \text{ km s}^{-1}$. The *blue dotted* (*red solid*) lines represent a model in which the supershell has a column density of $N_{\text{HI}} = 10^{21}$ ($N_{\text{HI}} = 10^{19}$) cm^{-2} and a maximum radius that is $r_{\text{sh}} = 0.1 \text{ kpc}$ ($r_{\text{sh}} = 1.0 \text{ kpc}$). Our calculations assume that there is no neutral gas (or dust) interior to the HI supershell.

The *left panel* of Figure 5 shows that inside the supershell the energy density decreases more gradually than r^{-2} because of photon trapping (similarly to the previously discussed cases in § 3.1–§ 3.2). The shell with the larger column of HI is more efficient at trapping the Ly α photons, and thus yields a flatter energy density profile. In both models the energy density drops steeply within the supershell (the energy density decreases as r^{-2} outside the shell, if no scattering occurs here).

The *right panel* of Figure 5 shows the ratio between the radiation and gravitational forces. Towards the center of the dark matter halo, baryons dominate the mass density and an evaluation of F_{grav} requires assumptions about the radial distribution of the baryons. For simplicity, we consider a fixed total mass interior to the supershell of $M(< r) = 10^8 M_{\odot}$, so that $F_{\text{grav}}(r) = GM(< r)m_p/r^2$. Note that any assumed mass profile $M(< r)$ will not affect the results as long as $F_{\text{rad}} \gg F_{\text{grav}}$.

We find that the radiation force exceeds gravity in both examples under consideration. For $N_{\text{HI}} = 10^{21} \text{ cm}^{-2}$ and $r_{\text{sh}} = 0.1 \text{ kpc}$, $F_{\text{rad}} \sim 10F_{\text{grav}}$. Thus, radiation pressure would have been important even if we had chosen $M \sim 10^9 M_{\odot}$. In the model with $N_{\text{HI}} = 10^{19} \text{ cm}^{-2}$ and

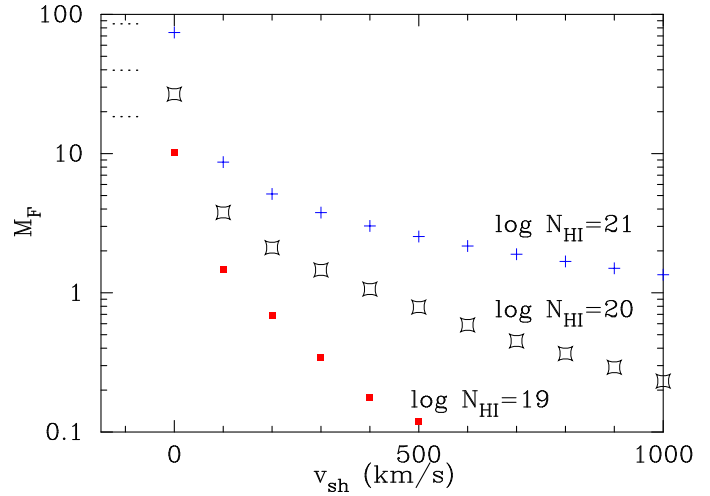


Figure 6. The multiplication factor M_F provides the total force that Ly α photons exert on a spherical HI shell, $F_{\text{tot}} = M_F L_{\alpha}/c$, where L_{α} is the Ly α luminosity of the source in erg s^{-1} and c is the speed of light. The plot shows M_F as a function of the expansion velocity of the HI shell, v_{sh} , for three values of HI column density, and under the assumption that the HI shell surrounds an empty cavity. The parameter M_F provides a measure of the efficiency by which Ly α photons can be ‘trapped’ by the shell of HI gas. Thus, M_F increases with increasing N_{HI} and decreasing v_{sh} . The *dotted horizontal lines* show the values of M_F that have been derived in the past (for a static, uniform, infinite slab of material e.g. Adams 1975).

$r_{\text{sh}} = 1.0 \text{ kpc}$, $F_{\text{rad}} \sim 10^2 F_{\text{grav}}$, and radiation pressure would have been important even if $M \sim 10^{10} M_{\odot}$. Hence, our calculations strongly suggest that Ly α radiation pressure may be dynamically important in the ISM of galaxies.

The *total* Ly α radiation force is obtained by summing the force over all atoms in the supershell. It is interesting to compare this force to L_{α}/c . The latter quantity denotes the total momentum transfer rate (force) from the Ly α radiation field to the supershell under the assumption that each Ly α photon is re-emitted isotropically after entering the shell (including multiple scatterings inside the supershell). In Figure 6 we plot the quantity M_F which is defined as

$$M_F \equiv \frac{\sum_{\text{atoms}} F_{\text{rad}}}{L_{\alpha}/c}, \quad (7)$$

as a function of the expansion velocity of the shell, v_{sh} for three different values of N_{HI} .

Figure 6 shows that M_F , which can be thought of as a force multiplication factor, greatly exceeds unity for low shell velocities and large HI column densities. The parameter M_F is related to the mean number of times that a Ly α photon ‘bounces’ back and forth between opposite sides of the expanding shell. For example, $M_F = 1$ when all Ly α photons enter the shell, scatter once, and then escape from the shell in no preferred direction. On the other hand, $M_F = 3$ when all Ly α photons enter the shell, scatter back towards the opposite direction, and then escape in no preferred direction after scattering in the shell for a second time. A schematic illustration of this argument is provided in Figure 7. Note that when $M_F = 1$ ($M_F = 3$), each photon spends on average a timescale of r_{sh}/c ($3r_{\text{sh}}/c$) in the bubble enclosed by the shell. In other words, the factor M_F relates to the ‘trap-

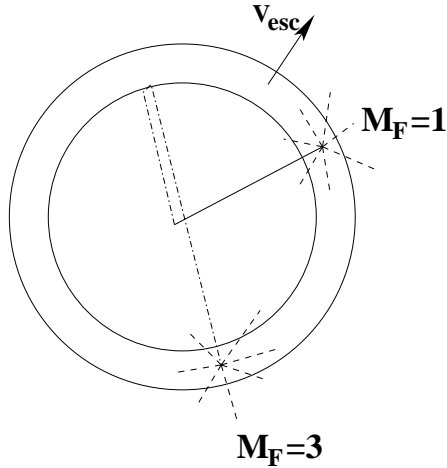


Figure 7. A schematic illustration of the origin of the force multiplication factor M_F in an expanding supershell. The $\text{Ly}\alpha$ source is located at the center of the expanding HI supershell. The *solid line* represents the trajectories of photons that enter the shell, scatter once, and then escape from the shell isotropically (indicated by the *dashed lines*). This corresponds to $M_F = 1$. On the other hand, the *dot-dashed line* represents the trajectories of photons that enter the shell, are scattered back in the opposite direction, and escape with no preferred direction after scattering in the shell for a second time. This corresponds to a case with $M_F = 3$. In general, $M_F = t_{\text{trap}}/(r_{\text{sh}}/c)$.

ping time', t_{trap} , that denotes the total time over which $\text{Ly}\alpha$ photons are trapped inside the supershell⁵ (see § 1) through the relation $M_F = t_{\text{trap}}/(r_{\text{sh}}/c)$. Indeed, when $v_{\text{sh}} \rightarrow 0$ we find that M_F reproduces the value $15(\tau_0/10^{5.5})$ (indicated by *horizontal dotted lines*) that was found by Adams (1975) and Bonilha et al. (1979) reasonably well (keeping in mind that these authors derived their result for a static, uniform, infinite slab of material, and assumed different frequency distributions for the emitted $\text{Ly}\alpha$ photons).

4 CONCLUSIONS

We have applied an existing Monte-Carlo $\text{Ly}\alpha$ radiative transfer code (described and tested extensively in Dijkstra et al. 2006) to the calculation of the pressure that is exerted by $\text{Ly}\alpha$ photons on an optically thick medium. This code enabled us to perform (the first) direct, accurate calculations of $\text{Ly}\alpha$ radiation pressure, which distinguishes this work from previous discussions on the importance of $\text{Ly}\alpha$ radiation pressure in various astrophysical environments.

⁵ This argument ignores the time spent on scattering inside the supershell itself. Photons penetrate on average an optical depth $\tau = 1$ into the shell. If this corresponds to a physical distance that is significantly smaller than the thickness of the shell (denoted by Δr_{sh}), then only a tiny fraction of the photons will diffuse through the shell. Hence, when averaged over these photons, ignoring the time spent inside the supershell itself is justified. Alternatively, photons with a mean free path that is at least comparable to the thickness of the shell, only spend a time $\sim \Delta r_{\text{sh}}/c \ll r_{\text{sh}}/c$ inside the supershell, which provides a negligible contribution to the trapping time.

We have focused on a range of models which represent galaxies at different cosmological epochs. In § 3.1 we have shown that the $\text{Ly}\alpha$ radiation pressure exerted on the neutral intergalactic medium (IGM) surrounding minihalos ($M_{\text{tot}} \sim 10^6 M_\odot$) in which the first stars form, can exceed gravity by 2–3 orders of magnitude (Fig 3), and in principle accelerate the gas in the IGM to tens of km s^{-1} . Thus, $\text{Ly}\alpha$ radiation pressure can launch supersonic winds in the IGM surrounding the first stars. Our analysis did not allow a detailed study of the consequences of these winds. A comprehensive study would require numerical simulations that capture the full IGM density field around minihalos in 3D and track the evolution of the shocks that may form in the IGM together with the $\text{Ly}\alpha$ radiative transfer. In this paper, we have also shown that $\text{Ly}\alpha$ radiation pressure is important in the neutral IGM that surrounds the HII regions produced by galaxies with a total halo mass of $M_{\text{tot}} = 10^8 M_\odot$ (Fig 4). These are the lowest mass, and hence the most abundant, halos in which gas can cool via atomic line excitation. Here, however, the absolute magnitude of the radiation force is too weak to drive the gas to supersonic velocities.

Finally, we have shown in § 3.3 that the $\text{Ly}\alpha$ radiation pressure exerted on neutral gas in the interstellar medium (ISM) of a galaxy can also have strong dynamical consequences. In particular, we have found that the $\text{Ly}\alpha$ radiation force exerted on an expanding HI supershell can exceed gravity by orders of magnitude (Fig 5), for reasonable assumptions about the gravitational force. It is therefore possible that $\text{Ly}\alpha$ radiation pressure plays an important role in determining the kinematics of HI supershells around starburst galaxies. We have demonstrated that the total $\text{Ly}\alpha$ radiation force on a spherical HI supershell can be written as $F_{\text{rad}} = M_F L_\alpha / c$, where the 'force-multiplication factor' M_F relates to the average trapping time of $\text{Ly}\alpha$ photons in the neutral medium. The factor M_F can greatly exceed unity, as illustrated by Fig 6. For comparison, the maximum possible radiation force due to continuum radiation⁶ is L_{bol}/c , in which L_{bol} is the bolometric luminosity of the central galaxy. For a typical star forming galaxy, $L_\alpha \sim 0.07 L_{\text{bol}}$ (e.g. Partridge & Peebles 1967), whereas for a galaxy that contains population III stars, $L_\alpha \sim 0.24 L_{\text{bol}}$ (Schaerer 2003). Hence, the $\text{Ly}\alpha$ radiation pressure can dominate the maximum possible continuum radiation pressure if $M_F \gtrsim 14$ (for a normal stellar population), a threshold which is easily exceeded at large column densities of relatively slow-moving HI shells (see Fig 6).

The important implication of our last result is that $\text{Ly}\alpha$ radiation pressure may drive outflows of HI gas in the ISM. Observations of local starburst galaxies have shown that the presence of outflowing HI gas may be required to avoid complete destruction of the $\text{Ly}\alpha$ radiation by dust and to allow its escape from the host galaxies (Kunth et al. 1998; Hayes et al. 2008; Ostlin et al. 2008; Atek et al. 2008). At high redshifts, the $\text{Ly}\alpha$ emission line of galaxies is often red-

⁶ In principle trapping of continuum photons by free electrons can result in a similar force multiplication factor. However, this requires electron column densities in excess of $N_e \gtrsim 10^{24} \text{ cm}^{-2}$, while the observed HI column densities in supershells are $N_{\text{HI}} \lesssim 10^{21} \text{ cm}^{-2}$, and no observational evidence exists that supershells predominantly consists of ionized gas.

shifted relative to other nebular recombination lines (such as H α) and metal absorption lines (e.g. Pettini et al. 2001; Shapley et al. 2003). Furthermore, the spectral shape of the Ly α emission line is typically asymmetric, with emission extending well into the red wing of the line (e.g. Lequeux et al. 1995). Both of these observations can be explained simultaneously if the observed Ly α photons scatter off neutral hydrogen atoms in an outflowing 'supershell' of HI gas that surrounds the star forming regions (Lequeux et al. 1995; Tenorio-Tagle et al. 1999; Ahn et al. 2003; Ahn 2004; Verhamme et al. 2006, 2008). The possibility that Ly α radiation pressure may be important in determining the properties of expanding supershells is exciting, and is discussed in more detail in a companion paper (Dijkstra & Loeb 2008).

Acknowledgments This work is supported by in part by NASA grant NNX08AL43G, by FQXi, and by Harvard University funds.

REFERENCES

- Abel, T., Norman, M. L., & Madau, P. 1999, ApJ, 523, 66
- Abel, T., Bryan, G. L., & Norman, M. L. 2002, Science, 295, 93
- Abel, T., Wise, J. H., & Bryan, G. L. 2007, ApJL, 659, L87
- Adams, T. F. 1975, ApJ, 201, 350
- Ahn, S.-H., & Lee, H.-W. 2002, Journal of Korean Astronomical
- Ahn, S.-H., Lee, H.-W., & Lee, H. M. 2003, MNRAS, 340, 863
- Ahn, S.-H. 2004, ApJL, 601, L25
- Atek, H., Kunth, D., Hayes, M., Ostlin, G., Mas-Hesse, J. M., & . 2008, ArXiv e-prints, 805, arXiv:0805.3501
- Barkana, R., & Loeb, A. 2001, Physics Reports, 349, 125
- Barkana, R. 2004, MNRAS, 347, 59
- Bithell, M. 1990, MNRAS, 244, 738
- Bonilha, J. R. M., Ferch, R., Salpeter, E. E., Slater, G., & Noerdlinger, P. D. 1979, ApJ, 233, 649
- Chandrasekhar, S. 1945, ApJ, 102, 402
- Chen, H.-W., Prochaska, J. X., & Gnedin, N. Y. 2007, ApJL, 667, L125
- Cox, D. P. 1985, ApJ, 288, 465
- Dijkstra, M., Haiman, Z., & Spaans, M. 2006, ApJ, 649, 14
- Dijkstra, M., Lidz, A., & Wyithe, J. S. B. 2007, MNRAS, 377, 1175
- Dijkstra, M., & Loeb, A. 2008, submitted to MNRAS
- Elitzur, M., & Ferland, G. J. 1986, ApJ, 305, 35
- Furlanetto, S. R., Zaldarriaga, M., & Hernquist, L. 2004, ApJ, 613, 1
- Gnedin, N. Y., Kravtsov, A. V., & Chen, H.-W. 2008, ApJ, 672, 765
- Haehnelt, M. G. 1995, MNRAS, 273, 249
- Haiman, Z., Thoul, A. A., & Loeb, A. 1996, ApJ, 464, 523
- Hayes, M., Ostlin, G., Mas-Hesse, J. M., & Kunth, D. 2008, ArXiv e-prints, 803, arXiv:0803.1176
- Heger, A., & Woosley, S. E. 2002, ApJ, 567, 532
- Heiles, C. 1984, ApJS, 55, 585
- Hui, L., & Gnedin, N. Y. 1997, MNRAS, 292, 27
- Kitayama, T., Yoshida, N., Susa, H., & Umemura, M. 2004, ApJ, 613, 631
- Komatsu, E., et al. 2008, ArXiv e-prints, 803, arXiv:0803.0547
- Kunth, D., Mas-Hesse, J. M., Terlevich, E., Terlevich, R., Lequeux, J., & Fall, S. M. 1998, A&A, 334, 11
- Lee, H.-W., & Ahn, S.-H. 1998, ApJL, 504, L61
- Lequeux, J., Kunth, D., Mas-Hesse, J. M., & Sargent, W. L. W. 1995, A&A, 301, 18
- Loeb, A., & Rybicki, G. B. 1999, ApJ, 524, 527 (LR99)
- Loeb, A. 2001, ApJL, 555, L1
- Maller, A. H., & Bullock, J. S. 2004, MNRAS, 355, 694
- McKee, C. F., & Tan, J. C. 2007, ArXiv e-prints, 711, arXiv:0711.1377
- McClure-Griffiths, N. M., Dickey, J. M., Gaensler, B. M., & Green, A. J. 2002, ApJ, 578, 176
- McQuinn, M., Lidz, A., Zahn, O., Dutta, S., Hernquist, L., & Zaldarriaga, M. 2007, MNRAS, 377, 1043
- Oh, S. P., & Haiman, Z. 2002, ApJ, 569, 558
- Osterbrock, D. E. 1989, *Astrophysics of gaseous nebulae and active galactic nuclei*, University of Minnesota, et al. Mill Valley, CA, University Science Books.
- Ostlin, G., Hayes, M., Kunth, D., Mas-Hesse, J. M., Leitherer, C., Petrosian, A., & Atek, H. 2008, ArXiv e-prints, 803, arXiv:0803.1174
- Ouchi, M., et al. 2008, ApJS, 176, 301
- Partridge, R. B., & Peebles, P. J. E. 1967, ApJ, 147, 868
- Pettini, M., Shapley, A. E., Steidel, C. C., Cuby, J.-G., Dickinson, M., Moorwood, A. F. M., Adelberger, K. L., & Giavalisco, M. 2001, ApJ, 554, 981
- Pritchard, J. R., & Loeb, A. 2008, ArXiv e-prints, 802, arXiv:0802.2102
- Rybicki, G. B., & Lightman, A. P. 1979, New York, Wiley-Interscience, 1979. 393 p.,
- Ryder, S. D., Staveley-Smith, L., Malin, D., & Walsh, W. 1995, AJ, 109, 1592
- Schaerer, D. 2002, A&A, 382, 28
- Schaerer, D. 2003, A&A, 397, 527
- Shapley, A. E., Steidel, C. C., Pettini, M., & Adelberger, K. L. 2003, ApJ, 588, 65
- Tenorio-Tagle, G., & Bodenheimer, P. 1988, ARA&A, 26, 145
- Tenorio-Tagle, G., Silich, S. A., Kunth, D., Terlevich, E., & Terlevich, R. 1999, MNRAS, 309, 332
- Verhamme, A., Schaerer, D., & Maselli, A. 2006, A&A, 460, 397
- Verhamme, A., Schaerer, D., Atek, H., & Tapken, C. 2008, ArXiv e-prints, 805, arXiv:0805.3601
- Wyithe, J. S. B., & Loeb, A. 2006, *Nature*, 441, 322
- Yoshida, N., Omukai, K., Hernquist, L., & Abel, T. 2006, ApJ, 652, 6